

Impact of Aquaporin-4 Channels on K^+ Buffering and Gap Junction Coupling in the Hippocampus

SUSAN STROHSCHHEIN,¹ KERSTIN HÜTTMANN,¹ SIEGRUN GABRIEL,² DEVIN K. BINDER,³ UWE HEINEMANN,² AND CHRISTIAN STEINHÄUSER^{1*}

¹Institute of Cellular Neurosciences, University of Bonn, Bonn, Germany

²Institute of Neurophysiology, Charité, Berlin, Germany

³Division of Biomedical Sciences, Center for Glial-Neuronal Interactions, University of California, Riverside, California

KEY WORDS

water channels; connexin; astrocyte; AQP4 knock out; dye coupling

ABSTRACT

Aquaporin-4 (AQP4) is the main water channel in the brain and primarily localized to astrocytes where the channels are thought to contribute to water and K^+ homeostasis. The close apposition of AQP4 and inward rectifier K^+ channels (Kir4.1) led to the hypothesis of direct functional interactions between both channels. We investigated the impact of AQP4 on stimulus-induced alterations of the extracellular K^+ concentration ($[K^+]_o$) in murine hippocampal slices. Recordings with K^+ -selective microelectrodes combined with field potential analyses were compared in wild type (wt) and AQP4 knockout (AQP4^{-/-}) mice. Astrocyte gap junction coupling was assessed with tracer filling during patch clamp recording. Antidromic fiber stimulation in the alveus evoked smaller increases and slower recovery of $[K^+]_o$ in the stratum pyramidale of AQP4^{-/-} mice indicating reduced glial swelling and a larger extracellular space when compared with control tissue. Moreover, the data hint at an impairment of the glial Na^+/K^+ ATPase in AQP4-deficient astrocytes. In a next step, we investigated the laminar profile of $[K^+]_o$ by moving the recording electrode from the stratum pyramidale toward the hippocampal fissure. At distances beyond 300 μ m from the pyramidal layer, the stimulation-induced, normalized increases of $[K^+]_o$ in AQP4^{-/-} mice exceeded the corresponding values of wt mice, indicating facilitated spatial buffering. Astrocytes in AQP4^{-/-} mice also displayed enhanced tracer coupling, which might underlie the improved spatial redistribution of $[K^+]_o$ in the hippocampus. These findings highlight the role of AQP4 channels in the regulation of K^+ homeostasis. © 2011 Wiley-Liss, Inc.

INTRODUCTION

Aquaporin-4 (AQP4) is the main water channel in the brain, primarily localized to astrocytes (Frigeri et al., 1995; Nielsen et al., 1997). Astrocytes also abundantly express Kir4.1 K^+ channels (Higashi et al., 2001; Poopasundaram et al., 2000; Seifert et al., 2009). Previous work revealed a close association of AQP4 with Kir4.1 K^+ channels and implicated functional coupling of both transmembrane proteins (Nagelhus et al., 2004). Since Kir channels in astrocytes are crucial for the redistribution of extracellular K^+ released during neuronal activity, AQP4 might play a role in spatial K^+ buffering. In

line with this suggestion, genetic deletion or mislocation of AQP4 produces hyperactivity and impaired regulation of stimulus-induced changes in the extracellular K^+ concentration ($[K^+]_o$) (Amiry-Moghaddam et al., 2003; Binder et al., 2006). These findings corroborated the view that AQP4 and Kir4.1 constitute a functional unit and that disturbed AQP4 expression produces dysfunction of Kir4.1 channels. However, subsequent studies provided evidence against this concept, by demonstrating AQP4-independent Kir4.1 channel function (Ruiz-Ederra et al., 2007; Zhang and Verkman, 2008). Hence, the mechanism(s) accounting for altered seizure dynamics and spatial K^+ buffering in AQP4 deficiency yet have to be identified. To better understand the role of AQP4 channels in K^+ buffering, here, we combined patch clamp and gap junction coupling analyses with $[K^+]_o$ recordings in acute hippocampal slices from wild type (wt) and AQP4-deficient mice.

MATERIALS AND METHODS

Studies were conducted with AQP4-deficient [AQP4^{-/-}; Aqp4^{tm1Ask}; backcrossed into CD1; Ma et al. (1997)] and CD1 wt mice, all aged 60–90 days (p. 60–90).

Extracellular Recordings

Extracellular recordings were performed as described (Wallraff et al., 2006). Mice were anesthetized using ether and decapitated; brains were removed and placed in ice-cold preparation solution containing (in millimolar): 87 NaCl, 2.5 KCl, 1.25 NaH₂PO₄, 7 MgCl₂, 0.5 CaCl₂, 25 NaHCO₃, 25 glucose, 25 sucrose, bubbled with 95% O₂/5% CO₂. Transversal brain slices (400 μ m) were prepared using a vibratome (Campden Instruments, Leicester, UK). Slices were transferred to an interface

Grant sponsor: DFG; Grant numbers: SFB TR3, TPC1, C7, C9, SPP 1172 SE774/3; Grant sponsor: EU; Grant numbers: FP6 EpiCure, FP7-202167 NeuroGLIA; Grant sponsor: Hertie Foundation.

*Correspondence to: Christian Steinhäuser, Institute of Cellular Neurosciences, University of Bonn, Sigmund Freud Str. 25, 53105 Bonn, Germany.
E-mail: christian.steinhaeuser@ukb.uni-bonn.de

Received 21 December 2010; Accepted 23 February 2011

DOI 10.1002/glia.21169

Published online 28 March 2011 in Wiley Online Library (wileyonlinelibrary.com).

chamber, perfused at 1.8 mL/min with artificial cerebrospinal fluid (ACSF) in a humidified atmosphere of 95% O₂/5% CO₂ (34°C). ACSF contained (in millimolar) 129 NaCl, 3 KCl, 1.8 MgSO₄, 2 CaCl₂, 10 glucose, 1.25 NaH₂PO₄, 21 NaHCO₃, bubbled with 95% O₂/5% CO₂. Before recording, 30 μM L-APV, 30 μM CNQX, and 5 μM bicuculline were added to suppress synaptic transmission, and slices were allowed to equilibrate for 20 min. Changes in [K⁺]_o and field potentials were measured at a depth of 100 μm with double-barreled K⁺-selective/reference microelectrodes. Electrodes were prepared and tested as described (Lux and Neher, 1973) and displayed voltage responses of 59 ± 0.3 mV (*n* = 19) per decade increase in [K⁺]_o. The ion-sensitive barrel was tip filled with Fluka 60031 ionophore (Neu-Ulm, Germany) and backfilled with 100 mM KCl; the reference barrel was filled with 150 mM NaCl. Using a custom-made amplifier equipped with negative capacitance compensation, the signal at the reference barrel was subtracted from that at the K⁺-selective barrel. This voltage signal was converted to K⁺ concentration using a modified Nernst equation: $\log[\text{Ion}]_1 = \frac{E_m}{s} (s \times v) \exp(-1) + \log[\text{Ion}]_0$, where E_m is the recorded potential, s the electrode slope obtained at calibration, v the valence of the specific ion, [Ion]₀ the ion concentration at rest, and [Ion]₁ the ion concentration during stimulation. Recording electrodes were placed at the border of stratum pyramidale and stratum oriens in the middle of the CA1 subfield. Bipolar stimulation electrodes (platinum wires, 20-μm diameter) were positioned in the alveus in CA1 (close to the subiculum) to elicit antidromic population spikes. We applied paired stimuli (0.1 ms, 50-ms interval) or trains of stimuli (10 s, 20 Hz), programmed with Master-8 (A.M.P.I., Jerusalem, Israel). Intensities were selected to evoke population spike amplitudes at 25, 50, 75, and 100% of maximal response. To obtain a laminar profile of changes in [K⁺]_o, we shifted the recording electrodes from the stratum pyramidale through radiatum toward the hippocampal fissure (step size of 100 μm, set with a micromanipulator; MPC-100; Sutter Instruments, Novato, CA). Data were recorded using Spike 2 software (Cambridge Electronic Design, Cambridge, UK) and sampled at 10 kHz (field potentials, 3-kHz filter) or 100 Hz ([K⁺]_o measurements, 1.6-Hz filter), respectively.

Patch-Clamp Analysis

Mice were anesthetized with isoflurane (DeltaSelect, London, UK) and decapitated. Brains were removed and 200-μm thick transverse slices were cut on a vibratome (VT1200S; Leica, Nussloch, Germany). During slicing, the tissue was submerged in ice-cold preparation solution (see "Extracellular Recordings" section). Thereafter, slices were maintained in the same solution at 35°C for 20 min, cooled down to room temperature, and placed for at least 30 min into ACSF containing (in millimolar): 126 NaCl, 3 KCl, 2 MgSO₄, 2 CaCl₂, 10 glucose, 1.25 NaH₂PO₄, 26 NaHCO₃, bubbled with 95% O₂/5% CO₂. Slices were transferred to a recording chamber and perfused with bubbled ACSF at room temperature. Cells

were visualized at 600-fold magnification with a microscope (Nikon Eclipse FN1, Amstelveen, The Netherlands). Whole-cell voltage-clamp recordings were obtained in visually identified "passive" astrocytes (Mathias et al., 2003; Steinhäuser et al., 1994) of the CA1 stratum radiatum. Pipettes (from borosilicate capillaries; Hilgenberg, Malsfeld, Germany) had resistances of 3–6 MΩ when filled with internal solution containing (in millimolar): 130 K-gluconate, 1 MgCl₂, 3 Na₂-ATP, 20 HEPES, 10 EGTA; pH 7.2. Currents were recorded with an EPC7 amplifier (HEKA Elektronik, Lambrecht, Germany). Data were stored on a computer using TIDA software (HEKA), filtered at 10 kHz, and sampled at 6 or 30 kHz. Only one astrocyte was recorded in any individual slice.

Evaluation of Gap Junctional Coupling

As a measure of gap junctional coupling, we used the extent of diffusion of a tracer, as previously described (Wallraff et al., 2004, 2006). To this end, *N*-biotinyl-L-lysine (biotin; Sigma, Taufkirchen, Germany) was added to the pipette solution (0.5%) and recordings from astrocytes in the stratum radiatum were limited to 19–22 min. After recording slices were fixed in 4% paraformaldehyde in 0.1 M phosphate-buffered saline (PBS), pH 7.4 at 4°C. The next steps were carried out at room temperature, unless otherwise stated. Slices were washed with PBS (0.1 M) and placed in blocking buffer (10% NGS, 2% Triton X-100 in 0.1 M PBS) for 2 h. Then the slices were incubated in 0.1 M PBS containing 1:100 streptavidin-Cy2 conjugate (Jackson ImmunoResearch, Newmarket, UK), 2% NGS, and 0.1% Triton X-100 overnight at 4°C on a shaker. On the next day, slices were washed (PBS), mounted in Vectashield (Vector Laboratories, Burlingame, CA), and inspected in a Zeiss Axiophot microscope (Zeiss, Oberkochen, Germany). Images were taken with a 20×/NA0.8 Plan Apochromat lens. A digital SPOT camera (Diagnostic Instruments, Sterling Heights, MI) and MetaVue software (Universal Imaging Corporation, West Chester, OH) were used to obtain image stacks (optical sections at 1-μm intervals) in two channels. Image analysis was performed with Fiji software.

Statistics

Data are expressed as mean ± SEM. Data obtained from different slices of a single animal were pooled to yield a single data point. Data were examined for statistical significance using two-tailed Student's *t*-test or two-way ANOVA. Covariance analysis was performed for comparison of regression curves. Differences were considered significant at *P* < 0.05.

RESULTS

Smaller Stimulus-Induced [K⁺]_o Elevations in the Hippocampus of AQP4^{-/-} Mice

In accordance with previous findings (Binder et al., 2006), baseline [K⁺]_o was not different in the hippocampus of wt vs. AQP4^{-/-} mice (3.0 ± 0.004 mM, *n* = 8 vs.

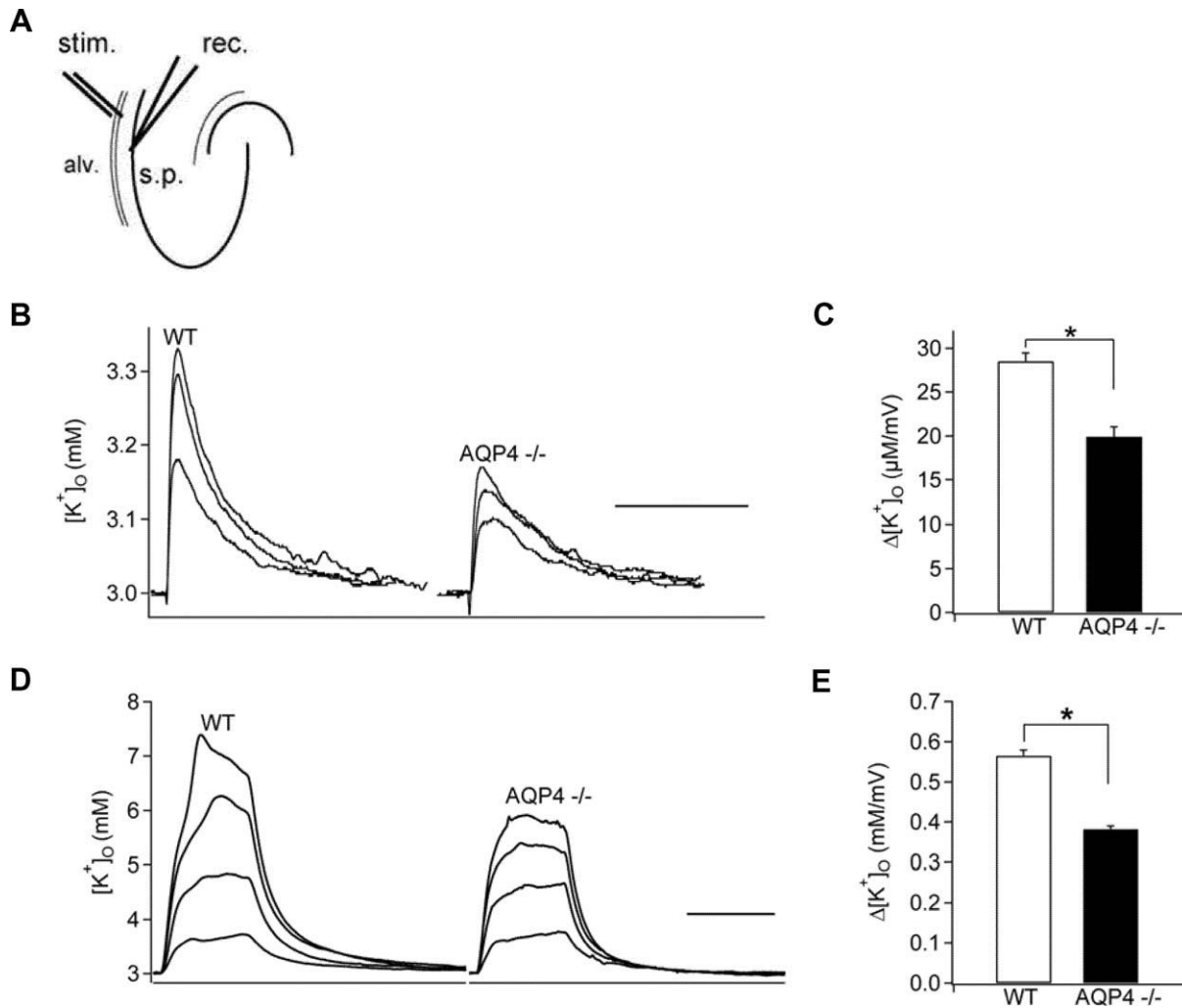


Fig. 1. Stimulation-induced $[K^+]_o$ changes in wt and $AQP4^{-/-}$ mice. **A:** The stimulation electrode (stim.) was placed in the alveus (alv.), the recording electrode (rec.) in the CA1 region, at the border between strata oriens and pyramidale (s.p.). **B:** Examples of $[K^+]_o$ responses to paired-pulse stimulation (0.1 ms, 50-ms interval) adjusted to evoke 50, 75, and 100% of maximum population spike amplitudes. **C:** Data were normalized to the corresponding population spikes and averaged (wt, $28.5 \pm 0.9 \mu\text{M}/\text{mV}$, $n = 10$ slices; six animals, open bars; $AQP4^{-/-}$

mice, $19.9 \pm 1.1 \mu\text{M}/\text{mV}$, $n = 5$ slices; five animals, full bars). **D:** Representative examples of $[K^+]_o$ responses elicited by stimulation trains (10 s, 20 Hz) at 25, 50, 75, and 100% of maximum stimulation intensity. **E:** Data were normalized to the corresponding population spike amplitudes and averaged. Open bar represents wt ($0.57 \pm 0.01 \text{ mM}/\text{mV}$, $n = 11$ slices; seven animals); full bars $AQP4^{-/-}$ mice ($0.38 \pm 0.01 \text{ mM}/\text{mV}$, $n = 7$ slices; five animals). Scale bars in (B,D): 10 s. Asterisks indicate statistically significant differences.

$2.9 \pm 0.04 \text{ mM}$, $n = 6$). To determine whether deletion of AQP4 affects local $[K^+]_o$ accumulation caused by neuronal activity, $[K^+]_o$ increases were evoked by antidromic stimulation of CA1 neurons (Fig. 1A). To obtain reproducible, temporally stable $[K^+]_o$ rises caused by action potentials of CA1 neurons, synaptic transmission was suppressed by applying antagonists for ionotropic glutamate and GABA receptors (Wallraff et al., 2006). Population spike amplitudes increased with stronger stimulation intensity but did not differ significantly between wt ($n = 11$ slices) and $AQP4^{-/-}$ mice ($n = 7$ slices), respectively (100% values: wt $8.0 \pm 0.9 \text{ mV}$; $AQP4^{-/-}$ mice $7.0 \pm 1.2 \text{ mV}$).

Paired-pulse stimulation (0.1 ms, 50-ms interval) was applied to the alveus with the stimulation intensity being set to elicit 50, 75, and 100% of maximal population spike amplitudes. This protocol generated reproduc-

ible increases in $[K^+]_o$, which were well above baseline noise (Fig. 1B). Consecutive responses to five paired pulses were averaged. To investigate $[K^+]_o$ rises independent of the level of neuronal activation, the increases in $[K^+]_o$ ($\Delta[K^+]_o$) were normalized to the respective population spike amplitudes. Two-way ANOVA revealed that (i) the normalized $\Delta[K^+]_o$ data were independent of stimulation intensity for both genotypes ($P = 0.16$; not shown) and (ii) stimulation induced significantly smaller normalized $[K^+]_o$ increases in $AQP4^{-/-}$ mice ($P = 0.001$). Pooled data are shown in Fig. 1C.

To compare K^+ buffering in wt and $AQP4^{-/-}$ mice during stronger K^+ load, we applied trains of stimuli evoking 25, 50, 75, or 100% of maximal population spikes. Even at 25% stimulus intensity, train-induced $[K^+]_o$ elevations were larger than any of the responses to double pulses (Fig. 1D). At maximal stimulation

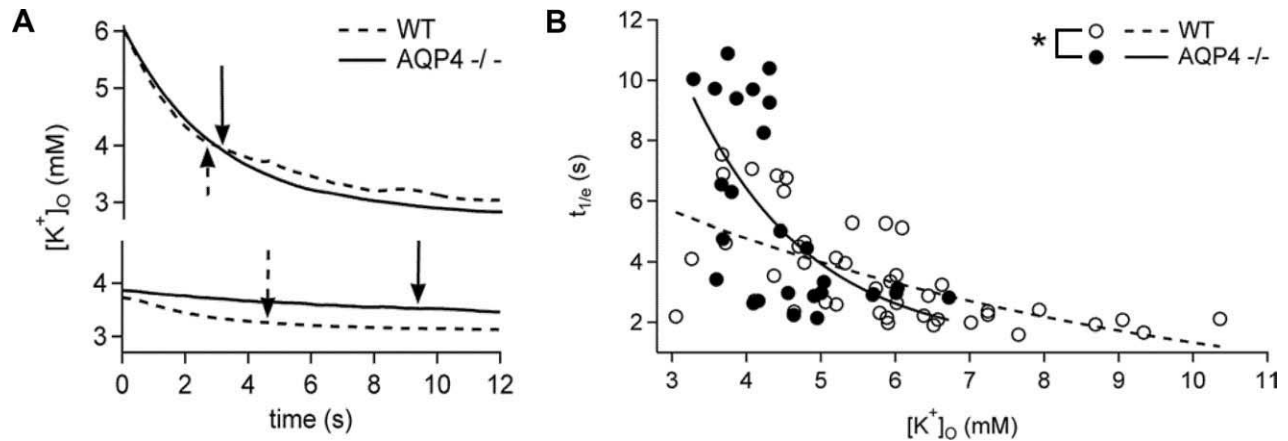


Fig. 2. Delayed recovery of stimulation-induced increase in $[K^+]_o$ in $AQP4^{-/-}$ mice. **A**: Decline of representative, matched $[K^+]_o$ transients after train stimulation (20 Hz) evoked with low (bottom; wt, 25%; $AQP4^{-/-}$, 50%) and high (top; 100%) stimulation intensity (wt, dotted line; $AQP4^{-/-}$, full line). Arrows indicate decline to 1/e of the initial amplitude. Note the slower decline at low stimulation in $AQP4^{-/-}$ tissue while at stronger stimulation both genotypes displayed similar recovery. **B**: Concentration dependence of $[K^+]_o$ recovery. $t_{1/e}$ values of both genotypes could be best approximated by exponential functions (dotted

and full lines). Covariance analysis after logarithmic transformation for linearization (wt: Pearson coefficient, $r = -0.64$, $n = 43$ pairs of variates; $AQP4^{-/-}$: $r = -0.61$, $n = 27$ pairs of variates) revealed different slopes (wt: -0.39 ; $AQP4^{-/-}$: -0.17 ; $F = 5.4$) and y-axis intercepts (wt: 8.8 s, $AQP4^{-/-}$: 27.6 s, $F = 497.2$), demonstrating that removal of moderate extracellular K^+ load (up to 4 mM) was significantly slowed in the absence of AQP4. No differences between genotypes were found at higher $[K^+]_o$.

intensity, $[K^+]_o$ did never exceed the “ceiling level” of 12 mM (Heinemann and Lux, 1977) in either genotype (all of 17 slices). Averaged maximal $[K^+]_o$ values evoked at 100% stimulation intensity (cf. Fig. 1B,D) did not differ significantly between wt (7.3 ± 0.6 mM, $n = 10$ slices, seven animals) and $AQP4$ -deficient mice (5.8 ± 0.4 mM, $n = 7$ slices, six animals; 100% stimulation intensity, respectively). Two-way ANOVA found no differences in normalized $[K^+]_o$ rise with increasing stimulation strength for the respective genotype ($P = 0.76$), but identified significantly smaller $\Delta[K^+]_o$ values in $AQP4^{-/-}$ mice ($P = 0.004$). Pooled data are depicted in Fig. 1E. Thus, AQP4 is equally important for regulation of K^+ homeostasis at very high K^+ levels (train stimulation) and at more physiological K^+ levels (paired-pulse stimulation).

Slower Recovery of $[K^+]_o$ After Neuronal Stimulation in $AQP4$ -Deficient Hippocampus

Previous data from the cortex reported faster diffusion in the extracellular space and delayed recovery from stimulus-induced $[K^+]_o$ elevations in $AQP4$ -deficient mice (Binder et al., 2004, 2006). To determine whether the K^+ equilibration time course was delayed in $AQP4^{-/-}$ mice, we analyzed the decay kinetics of $[K^+]_o$ after train stimulation (10 s, 20 Hz). For quantification, we determined the time at which $[K^+]_o$ had declined to 1/e of its maximal value ($t_{1/e}$) and plotted this parameter against peak $[K^+]_o$ values. The representative traces in Fig. 2A indicate that independent of the genotype, $t_{1/e}$ values were inversely correlated with increasing $[K^+]_o$ amplitudes. $t_{1/e}$ values were plotted against maximal $[K^+]_o$ values and approximated by exponential functions (Fig. 2B). Covariance analysis after logarithmic transformation for linearization revealed different slopes and

y-axis intercepts for the genotypes, demonstrating that removal of low or moderate extracellular K^+ load (up to 4 mM) was significantly slowed in the absence of AQP4. No differences between genotypes were found at higher $[K^+]_o$ values (Fig. 2B).

$[K^+]_o$ undershoots are transient events, probably due to neuronal K^+ uptake (Heinemann and Lux, 1975; Ransom et al., 2000). Comparing the amplitude of undershoots between genotypes revealed no significant difference (wt, 0.018 ± 0.002 mM/mM, $n = 9$ slices, seven animals, $AQP4^{-/-}$, 0.016 ± 0.003 mM/mM, $n = 7$ slices, five animals; train stimulation at 100%).

Enhanced Spatial K^+ Redistribution in $AQP4$ -Deficient Mice

To investigate the impact of AQP4 on spatial K^+ buffering the laminar profile of stimulus-induced rises in $[K^+]_o$ from the pyramidal layer toward the hippocampal fissure was determined (Gabriel et al., 1998; Wallraff et al., 2006). Seventy-five percent stimulation intensity (10-s trains, 20 Hz) was used to detect the expected, small $[K^+]_o$ changes at positions away from the excitation site, and changes of $[K^+]_o$ were normalized to the rise in the pyramidal layer. Corresponding field potentials are depicted in Fig. 3B. Population spikes elicited by antidromic stimulation steeply declined toward the stratum lacunosum-moleculare, both in wt and $AQP4^{-/-}$ mice, indicating similar propagation of dendritic action potentials in both genotypes. Figure 3C demonstrates that the redistribution of extracellular K^+ in wt ($n = 11$ slices; seven animals) and $AQP4^{-/-}$ mice ($n = 9$ slices; six animals) did not differ through the stratum radiatum. In contrast, 300–600 μ m away from the pyramidal layer stimulus-induced $[K^+]_o$ changes revealed more efficient relocation of K^+ in $AQP4$ -deficient hippocampus (Fig. 3C).

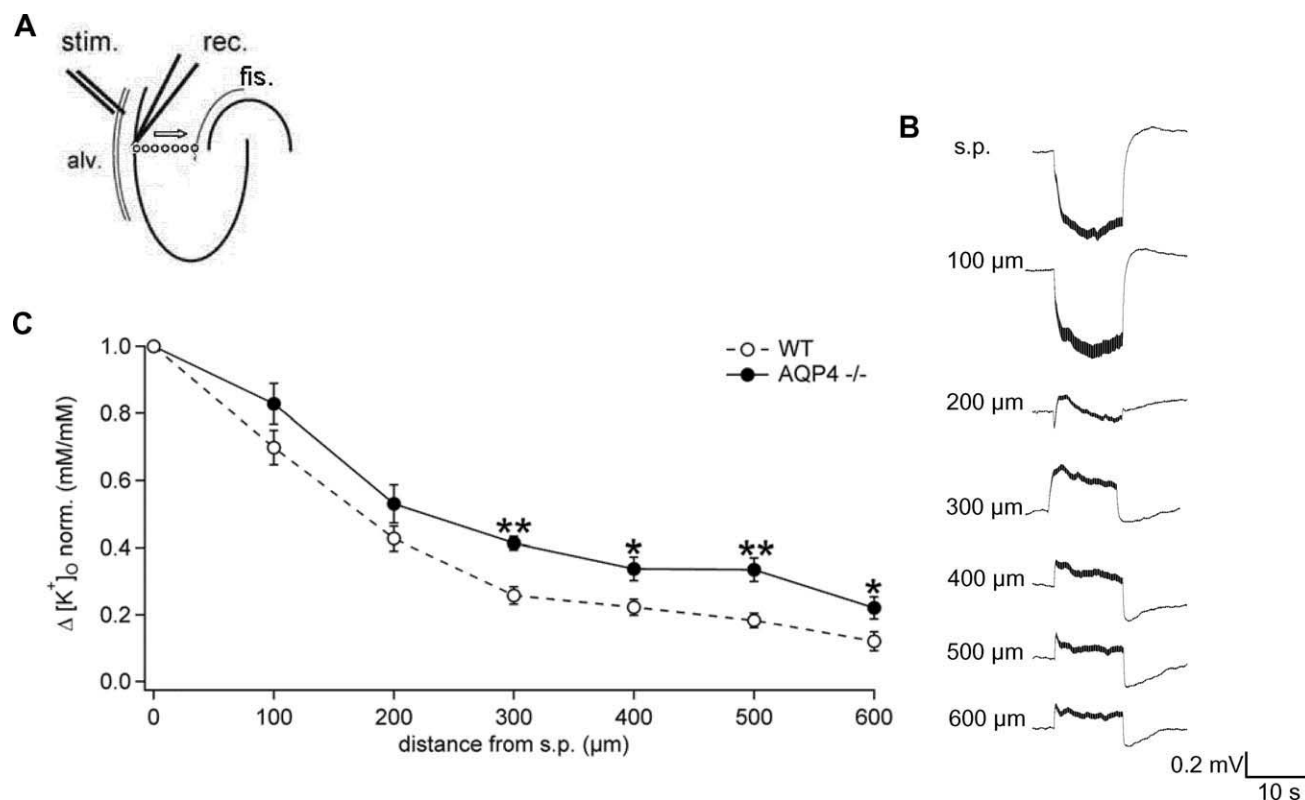


Fig. 3. Deletion of AQP4 improves spatial redistribution of K⁺ in the CA1 region. **A:** During alveus (alv.) stimulation (10 s, 20 Hz trains, 75% of maximal intensity, cf. Fig. 1A) the recording electrode (rec.) was stepped from the stratum pyramidale toward the hippocampal fissure (fis.) (step size, 100 μm). **B:** Representative examples of field potentials recorded in the CA1 region of an exemplary slice (distance from the

stratum pyramidale (s.p.) as indicated). **C:** Mean rises in [K⁺]_o were normalized to the rise in s.p., averaged (mean ± SEM) and plotted against the distance from the s.p. Open circles represent data from wt (*n* = 11 slices, seven animals), full circles from AQP4^{-/-} mice (*n* = 9 slices, six animals). Asterisks indicate significant differences between genotypes (**P* < 0.05, ***P* < 0.001).

Increased Tracer Coupling of Astrocytes in AQP4^{-/-} Mice

The data reported so far indicated smaller stimulus-induced increases and slower recovery of [K⁺]_o in the pyramidal layer of AQP4^{-/-} mice and enhanced redistribution of neuronally released K⁺ across the hippocampus. Next, we determined whether changes in gap junction coupling might have contributed to the changed K⁺ redistribution in AQP4-deficient mice. Astrocytes were selected with IR-DIC microscopy and filled with biocytin (*n* = 71) during whole cell recording. In both genotypes, all investigated cells displayed passive current patterns (resting potential -84.0 ± 2.9 mV; changes less than ± 2 mV during recording; not different between genotypes) (insets in Fig. 4A1,A2). Biocytin filling of single astrocytes in wt hippocampus revealed tracer spread to 66 cells on average while in AQP4^{-/-} mice the number was significantly larger (by 32%; Fig. 4B). Thus, AQP4-deficient astrocytes display increased gap junction coupling.

DISCUSSION

Although there is general agreement in the literature on a role of AQP4 in cerebral water balance and signal transduction, underlying mechanisms are disputed and previ-

ous findings have been conflicting. For example, AQP4 was reported to have a key role in maintaining blood-brain barrier integrity (Zhou et al., 2008), while a subsequent study demonstrated that AQP4 deletion does not produce significant structural abnormalities (Saadoun et al., 2009). Moreover, the close association of AQP4 with Kir4.1 gave rise to the hypothesis of functional coupling between both transmembrane proteins (Nagelhus et al., 2004), but later work was not in line with this concept (Ruiz-Ederra et al., 2007; Zhang and Verkman, 2008). Thus, AQP4 function in the brain is not well understood yet.

Here, we addressed the role of AQP4 in K⁺ buffering. In accordance with earlier work in the cortex *in vivo* (Binder et al., 2006), deletion of AQP4 did not influence baseline [K⁺]_o in the hippocampus, and we observed similar resting potentials in astrocytes of both genotypes. However, alveus stimulation produced smaller [K⁺]_o increases in the CA1 pyramidal layer of AQP4-deficient mice. Given that wt astrocytes rapidly and reversibly swell in response to elevation in [K⁺]_o (Risher et al., 2009) with an up to 30% decrease in extracellular space (Dietzel et al., 1980), these findings indicate concurrent movement of water and K⁺ through the membrane: In AQP4-deficient mice, water flux is reduced leading to enhanced extracellular space (Binder et al., 2004; Yao et al., 2008) and smaller [K⁺]_o elevations.

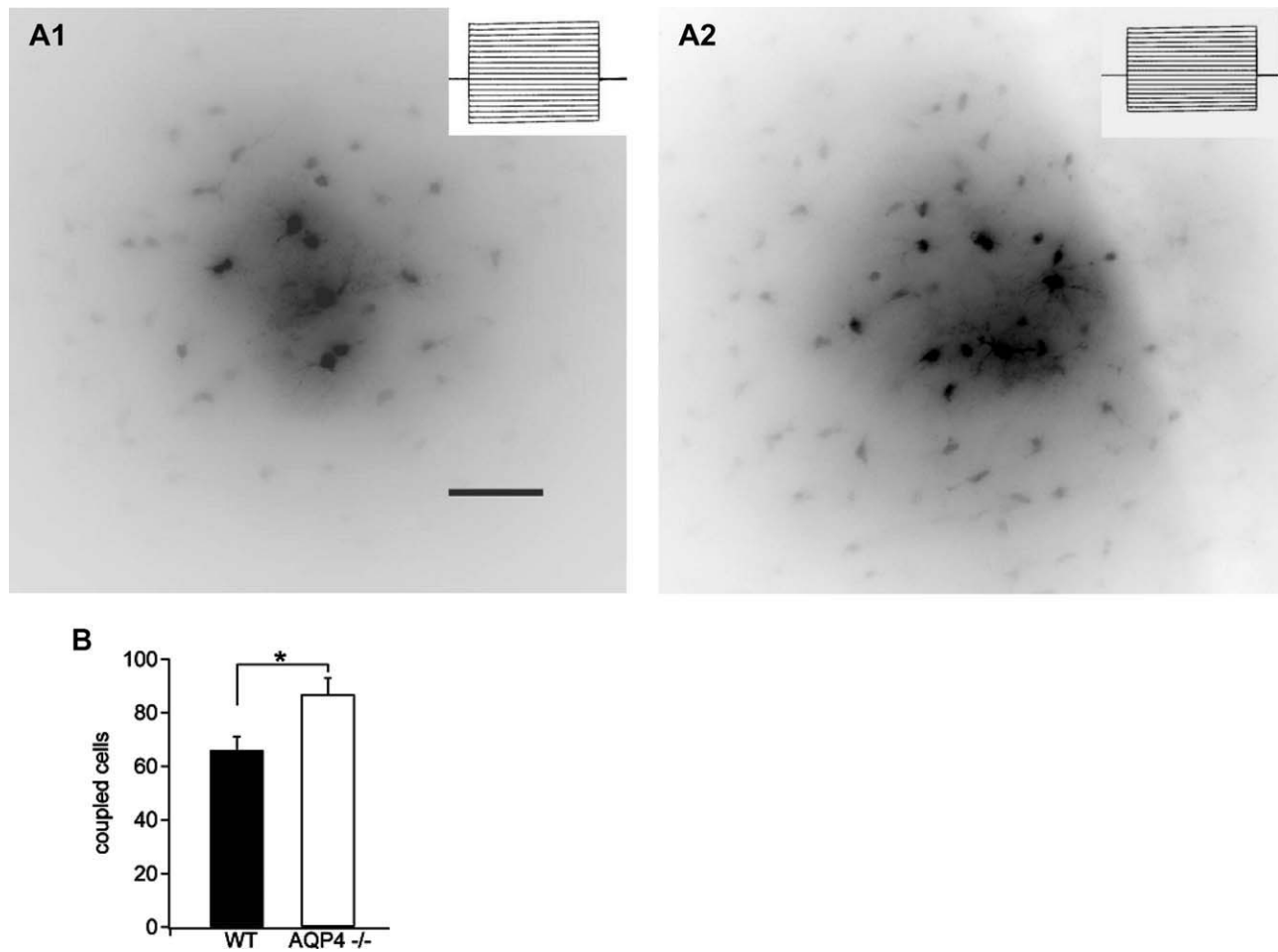


Fig. 4. Deletion of AQP4 enhances dye coupling in the hippocampus. Immunohistochemical visualization of tracer-coupled astrocytes in the CA1 stratum radiatum of wt (A1) and AQP4^{-/-} mice (A2). Astrocytes were filled with biocytin during whole cell recording. Current patterns are given in insets (responses to de- and hyperpolarization between -160 and $+20$ mV; 50 ms, holding potential -80 mV, 10 mV incre-

ments). Scale bar, 50 μ m. B: Summary of tracer filling experiments in wt (full bar; $n = 36$ filled cells from 10 animals) and AQP4^{-/-} mice (open bar; $n = 33$ filled cells from 6 animals). On average, the tracer spread to 66 ± 5 and 87 ± 6 cells in wt and AQP4^{-/-} mice, respectively. The difference between genotypes was statistically significant ($P < 0.05$).

The recovery kinetics of $[K^+]_o$ after stimulation revealed a concentration-dependent difference between genotypes. Moderate $[K^+]_o$ elevations (up to 4 mM) were followed by slowed K^+ reuptake in the absence of AQP4 but at higher $[K^+]_o$ loads similar time constants for K^+ removal were found in both genotypes. While global changes in K^+ recovery kinetics in the absence of AQP4 have been reported to occur in the cortex (Binder et al., 2006; Padmawar et al., 2005), our study specifically suggests a role for astroglial AQP4 channels in K^+ clearance kinetics under physiological conditions. Which mechanism(s) might underlie the concentration-dependent differences in K^+ reuptake kinetics? K^+ uptake and spatial buffering are critically dependent on Kir4.1 channels, which significantly contribute to the high K^+ resting conductance of astrocytes (Chever et al., 2010; Seifert et al., 2009; Tang et al., 2009). However, a recent study did not find major changes in astroglial Kir channel function in AQP4^{-/-} mice and argued that alternative mechanisms underlie the slowed K^+ reuptake previ-

ously reported (Zhang and Verkman, 2008). Besides spatial buffering, Na^+/K^+ pumps contribute to the clearance of K^+ during periods of elevated $[K^+]_o$. In the hippocampus, Na^+/K^+ pumps determine the recovery rate of $[K^+]_o$ during sustained high-frequency firing (D'Ambrosio et al., 2002). The glial Na^+/K^+ -ATPase isoform is highly sensitive to changes in $[K^+]_o$ around physiological K^+ concentrations (Rose and Ransom, 1996), while the neuronal isoform is insensitive to low $[K^+]_o$ alterations but senses changes in $[Na^+]_i$ (Rose and Ransom, 1997). Analyses of stimulus-induced $[K^+]_o$ dynamics in the optic nerve suggested that glial uptake instantaneously adjusts to changes in $[K^+]_o$, especially following weak stimulation. In contrast, the neuronal Na^+/K^+ -ATPase activates slower and has a larger role during sustained, strong neuronal activity (Ransom et al., 2000). On the basis of these findings, our data hint at impaired K^+ uptake through the glial Na^+/K^+ -ATPase in AQP4-deficient hippocampus. It is conceivable that lack of AQP4 directly affects Na^+/K^+ -ATPase func-

tion because both molecules form macromolecular complexes in astrocytes and probably functionally interact with each other (Illarionova et al., 2010). The neuronal Na⁺/K⁺-ATPase seems not to be impaired in AQP4^{-/-} mice because we observed similar amplitudes of the undershoot as in wt mice (Heinemann and Lux, 1975; Ransom et al., 2000).

Despite slightly impaired K⁺ reuptake, spatial buffering of K⁺ appeared to be more efficient in AQP4-deficient mice as revealed by analyzing laminar [K⁺]_o profiles. The differences in [K⁺]_o distant to the stimulation site might result from the increase in gap junction coupling among astrocytes lacking AQP4 we have found, because coupling is important for K⁺ redistribution in the hippocampus (Wallraff et al., 2006). Notably, an opposite regulation occurs in cultured murine astrocytes where AQP4 knockdown by siRNA-induced downregulation of Cx43 and junctional coupling (Nicchia et al., 2005). Culture conditions might account for these differences, although compensatory regulation of connexin(s) in constitutive AQP4^{-/-} mice cannot be excluded. The mechanism(s) underlying enhanced tracer spread in AQP4^{-/-} mice and the proposed functional link between connexins and AQP4 has still to be elucidated. In addition to changes in coupling, impaired ability of water to follow K⁺ efflux in AQP4^{-/-} astrocytes could cause elevated [K⁺]_o levels at remote sites (Dietzel et al., 1980).

In conclusion, our data demonstrate smaller stimulus-induced [K⁺]_o increases, enhanced K⁺ redistribution and elevated gap junction coupling of astrocytes in the hippocampus of AQP4^{-/-} mice. These changes might contribute to protection of the brain after insults, e.g., cytotoxic edema (Manley et al., 2000; Papadopoulos and Verkman, 2005). Given that AQP4 has various potential molecular interaction partners (Benfenati and Ferroni, 2010) more experimentation is needed to clarify its detailed role in controlling ion homeostasis.

ACKNOWLEDGMENTS

The authors gratefully acknowledge Alan Verkman (UCSF) for provision of AQP4^{-/-} mice, Ines Nauroth for comments on the manuscript, and Ina Fiedler for technical assistance.

REFERENCES

Amiry-Moghaddam M, Williamson A, Palomba M, Eid T, de Lanerolle NC, Nagelhus EA, Adams ME, Froehner SC, Agre P, Ottersen OP. 2003. Delayed K⁺ clearance associated with aquaporin-4 mislocalization: Phenotypic defects in brains of α -syntrophin-null mice. *Proc Natl Acad Sci USA* 100:13615–13620.

Benfenati V, Ferroni S. 2010. Water transport between CNS compartments: Functional and molecular interactions between aquaporins and ion channels. *Neuroscience* 168:926–940.

Binder DK, Papadopoulos MC, Haggie PM, Verkman AS. 2004. In vivo measurement of brain extracellular space diffusion by cortical surface photobleaching. *J Neurosci* 24:8049–8056.

Binder DK, Yao X, Zador Z, Sick TJ, Verkman AS, Manley GT. 2006. Increased seizure duration and slowed potassium kinetics in mice lacking aquaporin-4 water channels. *Glia* 53:631–636.

Chever O, Djukic B, McCarthy KD, Amzica F. 2010. Implication of kir4.1 channel in excess potassium clearance: An in vivo study on anesthetized glial-conditional kir4.1 knock-out mice. *J Neurosci* 30:15769–15777.

D'Ambrosio R, Gordon DS, Winn HR. 2002. Differential role of KIR channel and Na(+)/K(+)-pump in the regulation of extracellular K(+) in rat hippocampus. *J Neurophysiol* 87:87–102.

Dietzel I, Heinemann U, Hofmeier G, Lux HD. 1980. Transient changes in the size of the extracellular space in the sensorimotor cortex of cats in relation to stimulus-induced changes in potassium concentration. *Exp Brain Res* 40:432–439.

Frigeri A, Gropper MA, Umenishi F, Kawashima M, Brown D, Verkman AS. 1995. Localization of MIWC and GLIP water channel homologs in neuromuscular, epithelial and glandular tissues. *J Cell Sci* 108(Pt 9):2993–3002.

Gabriel S, Kivi A, Eilers A, Kovács R, Heinemann U. 1998. Effects of barium on stimulus-induced rises in [K⁺]_o in juvenile rat hippocampal area CA1. *NeuroReport* 9:2583–2587.

Heinemann U, Lux HD. 1975. Undershoots following stimulus-induced rises of extracellular potassium concentration in cerebral cortex of cat. *Brain Res* 93:63–76.

Heinemann U, Lux HD. 1977. Ceiling of stimulus induced rises in extracellular potassium concentration in the cerebral cortex of cat. *Brain Res* 120:231–249.

Higashi K, Fujita A, Inanobe A, Tanemoto M, Doi K, Kubo T, Kurachi Y. 2001. An inwardly rectifying K(+) channel, Kir41, expressed in astrocytes surrounds synapses and blood vessels in brain. *Am J Physiol Cell Physiol* 281:C922–C931.

Illarionova NB, Gunnarson E, Li Y, Brismar H, Bondar A, Zelenin S, Aperia A. 2010. Functional and molecular interactions between aquaporins and Na,K-ATPase. *Neuroscience* 168:915–925.

Lux HD, Neher E. 1973. The equilibration time course of (K⁺)_o in cat cortex. *Exp Brain Res* 17:190–205.

Ma T, Yang B, Gillespie A, Carlson EJ, Epstein CJ, Verkman AS. 1997. Generation and phenotype of a transgenic knockout mouse lacking the mercurial-insensitive water channel aquaporin-4. *J Clin Invest* 100:957–962.

Manley GT, Fujimura M, Ma T, Noshita N, Filiz F, Bollen AW, Chan P, Verkman AS. 2000. Aquaporin-4 deletion in mice reduces brain edema after acute water intoxication and ischemic stroke. *Nat Med* 6:159–163.

Matthias K, Kirchhoff F, Seifert G, Hüttmann K, Matyash M, Kettenmann H, Steinhäuser C. 2003. Segregated expression of AMPA-type glutamate receptors and glutamate transporters defines distinct astrocyte populations in the mouse hippocampus. *J Neurosci* 23:1750–1758.

Nagelhus EA, Mathiesen TM, Ottersen OP. 2004. Aquaporin-4 in the central nervous system: Cellular and subcellular distribution and coexpression with KIR4.1. *Neuroscience* 129:905–913.

Nicchia GP, Srinivas M, Li W, Brosnan CF, Frigeri A, Spray DC. 2005. New possible roles for aquaporin-4 in astrocytes: Cell cytoskeleton and functional relationship with connexin43. *FASEB J* 19:1674–1676.

Nielsen S, Nagelhus EA, Amiry-Moghaddam M, Bourque C, Agre P, Ottersen OP. 1997. Specialized membrane domains for water transport in glial cells: High-resolution immunogold cytochemistry of aquaporin-4 in rat brain. *J Neurosci* 17:171–180.

Padmawar P, Yao X, Bloch O, Manley GT, Verkman AS. 2005. K⁺ waves in brain cortex visualized using a long-wavelength K⁺-sensing fluorescent indicator. *Nat Methods* 2:825–827.

Papadopoulos MC, Verkman AS. 2005. Aquaporin-4 gene disruption in mice reduces brain swelling and mortality in pneumococcal meningitis. *J Biol Chem* 280:13906–13912.

Poopalasundaram S, Knott C, Shamotienko OG, Foran PG, Dolly JO, Ghiani CA, Gallo V, Wilkin GP. 2000. Glial heterogeneity in expression of the inwardly rectifying K⁺ channel, Kir41, in adult rat CNS. *Glia* 30:362–372.

Ransom CB, Ransom BR, Sontheimer H. 2000. Activity-dependent extracellular K⁺ accumulation in rat optic nerve: The role of glial and axonal Na⁺ pumps. *J Physiol (London)* 522:427–442.

Risher WC, Andrew RD, Kirov SA. 2009. Real-time passive volume responses of astrocytes to acute osmotic and ischemic stress in cortical slices and in vivo revealed by two-photon microscopy. *Glia* 57:207–221.

Rose CR, Ransom BR. 1996. Intracellular sodium homeostasis in rat hippocampal astrocytes. *J Physiol (London)* 491:291–305.

Rose CR, Ransom BR. 1997. Regulation of intracellular sodium in cultured rat hippocampal neurons. *J Physiol (London)* 499:573–587.

Ruiz-Ederra J, Zhang H, Verkman AS. 2007. Evidence against functional interaction between aquaporin-4 water channels and Kir4.1 K⁺ channels in retinal muller cells. *J Biol Chem* 282:21866–21872.

- Saadoun S, Tait MJ, Reza A, Davies DC, Bell BA, Verkman AS, Papadopoulos MC. 2009. AQP4 gene deletion in mice does not alter blood-brain barrier integrity or brain morphology. *Neuroscience* 161:764–772.
- Seifert G, Hüttmann K, Binder DK, Hartmann C, Wyczynski A, Neusch C, Steinhäuser C. 2009. Analysis of astroglial K⁺ channel expression in the developing hippocampus reveals a predominant role of the Kir4.1 subunit. *J Neurosci* 29:7474–7488.
- Steinhäuser C, Jabs R, Kettenmann H. 1994. Properties of GABA and glutamate responses in identified glial cells of the mouse hippocampal slice. *Hippocampus* 4:19–36.
- Tang X, Taniguchi K, Kofuji P. 2009. Heterogeneity of Kir4.1 channel expression in glia revealed by mouse transgenesis. *Glia* 57:1706–1715.
- Wallraff A, Kohling R, Heinemann U, Theis M, Willecke K, Steinhäuser C. 2006. The impact of astrocytic gap junctional coupling on potassium buffering in the hippocampus. *J Neurosci* 26:5438–5447.
- Wallraff A, Odermatt B, Willecke K, Steinhäuser C. 2004. Distinct types of astroglial cells in the hippocampus differ in gap junction coupling. *Glia* 48:36–43.
- Yao X, Hrabetova S, Nicholson C, Manley GT. 2008. Aquaporin-4-deficient mice have increased extracellular space without tortuosity change. *J Neurosci* 28:5460–5464.
- Zhang H, Verkman AS. 2008. Aquaporin-4 independent Kir4.1 K⁺ channel function in brain glial cells. *Mol Cell Neurosci* 37:1–10.
- Zhou J, Kong H, Hua X, Xiao M, Ding J, Hu G. 2008. Altered blood-brain barrier integrity in adult aquaporin-4 knockout mice. *NeuroReport* 19:1–5.